

Available online at [www.sciencedirect.com](http://www.sciencedirect.com)

ScienceDirect

journal homepage: [www.e-jmii.com](http://www.e-jmii.com)

Original Article

# Prophylactic intranasal administration of lipid nanoparticle formulated siRNAs reduce SARS-CoV-2 and RSV lung infection

Aroon Supramaniam<sup>a,b,1</sup>, Yaman Tayyar<sup>a,b,c,1</sup>,  
 Daniel T.W. Clarke<sup>b</sup>, Gabrielle Kelly<sup>a,b</sup>, Dhruba Acharya<sup>a</sup>,  
 Kevin V. Morris<sup>a,b</sup>, Nigel A.J. McMillan<sup>a,b,3</sup>, Adi Idris<sup>a,b,d,3,\*</sup>

<sup>a</sup> Menzies Health Institute Queensland, Griffith University, Southport, Queensland, Australia

<sup>b</sup> School of Pharmacy and Medical Science, Griffith University, Southport, Queensland, Australia

<sup>c</sup> Prorenata Biotech, Molendinar, Queensland, Australia

<sup>d</sup> School of Biomedical Sciences, Queensland University of Technology, Gardens Point, Queensland, Australia

Received 25 August 2022; received in revised form 17 November 2022; accepted 28 February 2023

Available online 8 March 2023



## KEYWORDS

SARS-CoV-2;  
 siRNA;  
 RSV;  
 LNP;  
 COVID-19;  
 Intranasal

**Abstract** RNA interference (RNAi) is an emerging and promising therapy for a wide range of respiratory viral infections. This highly specific suppression can be achieved by the introduction of short-interfering RNA (siRNA) into mammalian systems, resulting in the effective reduction of viral load. Unfortunately, this has been hindered by the lack of a good delivery system, especially via the intranasal (IN) route. Here, we have developed an IN siRNA encapsulated lipid nanoparticle (LNP) *in vivo* delivery system that is highly efficient at targeting severe acute respiratory syndrome coronavirus 2 (SARS-CoV-2) and respiratory syncytial virus (RSV) lung infection *in vivo*. Importantly, IN siRNA delivery without the aid of LNPs abolishes anti-SARS-CoV-2 activity *in vivo*. Our approach using LNPs as the delivery vehicle overcomes the significant barriers seen with IN delivery of siRNA therapeutics and is a significant advancement in our ability to deliver siRNAs. The study presented here demonstrates an attractive alternate delivery strategy for the prophylactic treatment of both future and emerging respiratory viral diseases.

Copyright © 2023, Taiwan Society of Microbiology. Published by Elsevier Taiwan LLC. This is an open access article under the CC BY license (<http://creativecommons.org/licenses/by/4.0/>).

\* Corresponding author. Menzies Health Institute Queensland, Building G05, Room 3.37a, Gold Coast Campus Griffith University, Queensland 4222, Australia.

E-mail address: [a.idris@griffith.edu.au](mailto:a.idris@griffith.edu.au) (A. Idris).

<sup>1</sup> Authors contributed equally to this work.

<sup>3</sup> Authors share senior authorship.

## Introduction

The novel coronavirus disease 2019 (COVID-19) caused by severe acute respiratory syndrome coronavirus 2 (SARS-CoV-2) has a mortality rate of ~2.0%.<sup>1</sup> Despite the deployment of several vaccines, SARS-CoV-2 variants continue to emerge, and there remains a need for a direct acting antiviral. Similarly, direct acting antivirals against another emerging respiratory virus, respiratory syncytia virus (RSV) are also needed. RSV is the most common cause of bronchiolitis and pneumonia in children over 1 year of age. Research towards effective treatment and a vaccine against RSV has been ongoing for nearly five decades with little success. Current treatments for RSV including palivizumab (for high-risk children) and ribavirin<sup>2</sup> are limited and have poor efficacy resulting in a supportive rather than curative approach. Twenty months into the COVID-19 pandemic, we have only seen the first oral antiviral drug, molnupiravir, that shortens time to clearance of SARS-CoV-2<sup>3</sup> and if administered early following infection, can reduce hospitalisation and death. With the advent of RNA biologics during the COVID-19 pandemic era and its rapid speed of development (e.g., Moderna mRNA-based COVID-19 vaccines<sup>4</sup>), there has been a strong impetus for the development of RNA-based therapeutics for a range of human diseases.<sup>5</sup>

RNA interference (RNAi) technology platform is rapidly regaining interest in the field of RNA biologics. As RNAi is modular and facile this approach could be applied to any virus of concern. RNAi works via the introduction of small interfering RNAs (siRNAs) that specifically target the protein-coding mRNAs via sequence complementarity, causing their subsequent degradation.<sup>6</sup> RNAi is potentially cost effective, scalable and can be easily programmed to target any viral RNA in a matter of days. However, the greatest challenge is their delivery, which is particularly difficult when targeting the respiratory tract. We have recently demonstrated that siRNAs complexed in lipid nanoparticles (LNPs) designed to highly conserved regions of SARS-CoV-2 give potent viral lung repression *in vivo* when delivered intravenously (IV).<sup>7</sup> Given the limited clinical utility for delivering siRNA via IV, here we aim to develop an intranasal (IN) siRNA therapy targeting SARS-CoV-2 and RSV. This serves as a more clinically tractable way of ameliorating virus infection in the lungs. We hypothesize that RNAi can be deployed as a prophylactic therapy to treat these viral infections using IN delivery approaches that target the respiratory epithelium suitable for outpatient use. Indeed, siRNA therapies against RSV have been attempted by Alnylam Pharmaceuticals with ALN-RSV01, a nasal spray formulation of a single naked siRNA directed against RSV nucleocapsid (N) protein gene.<sup>8</sup> Similarly for SARS-CoV-2, there is precedence for this approach as IN delivery of naked<sup>9</sup> and dendrimer formulated<sup>10</sup> siRNAs are successful at ameliorating SARS-CoV-2 infectious load in lungs of infected animals. Here, we formulated previously designed siRNAs targeting SARS-CoV-2<sup>7</sup> and an RSV-targeting siRNA in LNPs for IN delivery. The results presented here demonstrate that prophylactic IN delivered LNP-complexed siRNAs effectively and significantly reduce SARS-CoV-2 and RSV lung infection *in vivo*.

## Materials and methods

### Cell culture

Vero E6 cells were maintained in complete media; DMEM (Gibco-Invitrogen, Waltham, MA) supplemented with 10% heat inactivated fetal bovine serum (FBS) (30 min at 56 °C, Gibco-Invitrogen, Waltham, MA) and 1% of antibiotic/glutamine preparation (100 U/ml penicillin G, 100 U/ml streptomycin sulphate, and 2.9 mg/mL of L-glutamine) (Gibco-Invitrogen, Waltham, MA). A549 cells were maintained in complete media; DMEM/F12 (Gibco-Invitrogen, Waltham, MA) supplemented with 10% heat inactivated fetal bovine serum (FBS) (30 min at 56 °C, Gibco-Invitrogen, Waltham, MA) and 1% of antibiotic/glutamine preparation (100 U/ml penicillin G, 100 U/ml streptomycin sulphate, and 2.9 mg/mL of L-glutamine) (Gibco-Invitrogen, Waltham, MA).

### Chemicals, lipids, and reagents

Cyclophosphamide was obtained from Sigma–Aldrich (St. Louis, MO). Dioleoyl trimethylammonium propane (DOTAP), dioleoylphosphatidylethanolamine (DOPE), 1,2-distearoyl-sn-glycero-3-phosphocholine (DSPC), Polyethylene Glycol (PEG)2000-C16 Ceramide conjugate, and cholesterol were purchased from Sigma–Aldrich (St Louis, MI). D-Lin-MC3-DMA (MC3) was purchased from MedChemExpress (NJ, USA).

### siRNAs

Target sequences for siRNAs are listed in Table 1. All *in vitro* siRNAs were synthesized by Integrated DNA Technologies (IDT) (Coralville, IA, USA). siMod-UTR3 was designed as previously done<sup>7</sup> and synthesized by IDT (Coralville, IA, USA) as an RNA duplex. HPLC purified and high quantity siRNAs for *in vivo* work, siUTR3, siHel2, siN367 were synthesized by the RNA/DNA Synthesis core at the City of Hope (Duarte, CA), whereas siP, siScrM7 and siGFP were either synthesized by GenePharma (Shanghai, China) or IDT (Coralville, IA, USA). siGLO Red was purchased from Dharmacon™ (Lafayette, CO).

### Viruses

SARS-CoV-2 VOCs (Wuhan (Ancestral) – VIC1, B.1.351 (Beta) - VIC18383, B.1.617 (Kappa) - VIC18447, B.1.617.2 (Delta) - VIC18440, B.1.1.529 (Omicron) (BA.1 sub variant) - VIC35864) were obtained from the Peter Doherty Institute for Infection and Immunity and Melbourne Health, Victoria, Australia and cultured in Vero E6 cells. Viral supernatant was concentrated in Amicon® Ultra-15 Centrifugal Filter units (Merck, Germany) and viral titre determined by the viral immunoplaque assay. RSV strain A2 (RSV-A2) was obtained from Professor Paul Young (School of Chemistry and Molecular Biosciences, The University of Queensland, QLD, Australia). RSV-A2 was cultured in A549 cells, ultracentrifuged, and purified on a sucrose gradient before determining viral titre using a viral plaque assay.

**Table 1** siRNA and D-siRNA sequences used in this study.

siRNA	RNA sequence sense (5'-3')	RNA sequence antisense (5'-3')
siHel2	rAcrCrUrUrArUrArUrUrCrArCrArGrArArUrGrCrUrGUA	rUrArCrArGrCrArUrUrCrUrGrUrGrArArUrUrArArGrGrUrGfA
siUTR3	rArUrArCrUrUrCrCrArGrUrArArArArArArArArArCrCrAAC	rGrUrUrGrUrUrUrUrGrUrArArCrUrGrGrArArGrGrUrArUrArA
siMod-URT3	rAmUmArCmCmUrUrCrCrCmArGrUrAmAmCrA*TA*mArCrAAC	rG*UrUrGrUrUrUrGrUmUmAmCrUrGrGrArArGrGmUrAmUmArA
siP	rUrCrUrArGrArUrUrGrArArArArGrGrArArATT	rArArTrTrGrCrCrUrUrUrArUrUrGrArUrUrCrUrArGrGrArArU
siScrM7	rCrGrUrUrArUrCrGrCrGrUrUrArUrArUrArCrGrCrGrUAT	rArUrArCrGrCrGrUrUrUrArUrArCrGrCrGrArUrUrArArCrGrArC
siN367	rCrUrGrArCrUrUrUrGrGrArUrGrUrGrUrCrUrUJC	rUrGrGrArArArGrUrCrCrCrArGrCrGrGrArArArG
siGFP	rGrCrArCrGrArCrUrUrUrCrArArGrUrCrCrUrU	GGACUUGAAGAAGUCGUGCUU

RNA bases denoted with r; DNA bases are capitalized; 2'OME RNA is denoted with m; PS linkage is denoted with \*.

### Cell transfections

Cells were seeded overnight to 70–80% confluency before transfecting nucleic acids with either FuGENE 6 (Promega, Madison, WI) or Lipofectamine 2000 (Gibco-Invitrogen, Waltham, MA) in OptiMEM (Gibco-Invitrogen, Waltham, MA) as per manufacturer’s protocol.

### Viral plaque and immunoplaque assay

For SARS-CoV-2 viral plaque assays, Vero E6 cells were infected with a MOI 0.002 (250 plaque forming units (PFU)) of SARS-CoV-2 for 1hr before overlaying with 1% methylcellulose-viscosity (4000 centipoises) (Sigma–Aldrich, St. Louis, MO). Cells were incubated for 4 days at 37 °C before fixing in 8% formaldehyde and stained with 1% crystal violet to visualize plaques. Viral immunoplaque assays for SARS-CoV-2 were performed on Vero E6 cells as described previously<sup>11</sup> using recombinant monoclonal antibodies that recognize SARS-CoV-2 (CR3022). Antibodies were obtained from Dr Naphak Modhiran and Associate Professor Dan Watterson (School of Chemistry and Molecular Biosciences, The University of Queensland, QLD, Australia). Viral immunoplaque assays for RSV-A2 were performed on A549 cells using anti-RSV-F rabbit polyclonal sera. Anti-RSV sera was obtained from Professor Paul Young (School of Chemistry and Molecular Biosciences, The University of Queensland, QLD, Australia).

### RSV viral RNA load determination

A549 cells were seeded in 24 well plates and incubated overnight at 37 °C. Cells were then transfected with siRNAs using Oligofectamine (Gibco-Invitrogen, Waltham, MA) overnight before infecting with RSV-A2 (MOI = 0.001). RNA was then extracted from cells after 48 h. Total RNA was purified from cell cultures using standard protocols including initial lysing with Trizol (Gibco-Invitrogen, Waltham, MA). qPCR was performed on the QIAGEN Rotor-gene (QIAGEN, Germany) using the GoTaq qPCR master mix (Promega, WI) with gene of interest primers specific for the RSV P gene A/C, 5'- TGAATTCATGGAGAAGATGC-3' (sense) and 5'- AGGGCTTCTTTGGTTACTTCT-3' (antisense), whereas reference gene primers were specific for human lamin A/C, 5'- TGGAGATGATCCCTTGCTGA-3' (sense) and 5'- GCATGGCCACTTCTCCCA-3' (antisense).

### sLNP synthesis

Nucleic acid-entrapped PEGylated lipid particles were prepared as previously described.<sup>12</sup> Briefly, required amounts of DOTAP, cholesterol, DOPE, and PEG2000-C16 Ceramide were dissolved individually in tert-butanol before being mixed at a molar ratio of 50:35:5:10. The required amounts of siRNA were dissolved in sucrose containing water (sucrose amount was calculated to generate an isotonic solution at the final step). A nitrogen: phosphate (N/P) ratio of four was generated by mixing the solutions mentioned above (1:1 v/v) to formulate the co-solvent system before the mixture was snap-frozen and freeze-dried (Alpha 1–2 LDplus, Martin Christ, Germany) at

0.05 mbar overnight. The freeze-dried matrix was then hydrated with sterile nuclease free water to the required concentration. Nanoparticles were then filtered through a 0.45 µm filter and stored at 4 °C. The mixture was left at room temperature for 2 h prior to characterization.

### dmLNP synthesis

Lipids were prepared at a 40:25:10:22:3 (DOTAP:MC3:DSPC:Chol:PEG) molar ratio. Lipids in ethanol were mixed with siRNAs in an aqueous phase at a mol cationic lipid: mol RNA (N:P) ratio of 3:1 using the NanoAssemblr Benchtop machine (Precision NanoSystems; Vancouver, BC, Canada). This machine contains a microfluidic chip by which the injected lipids and nucleic acids are mixed rapidly in a staggered herringbone pattern at a total flow rate of 12 mL/min. The controlled mixing of the aqueous and organic streams produces homogeneous nanoparticles. Immediately following the mixing process, the nanoparticles were diluted 1:4 with 1xPBS to reduce the amount of ethanol present in solution. The nanoparticle solution was further diluted with 1xPBS up to 15 mL and then concentrated in a 100 kDa Amicon ultra-15 filter (Millipore; Burlington, MA, USA) via centrifugation at 400g for 120min. The flow through was discarded and another 15 mL 1xPBS was added to the column and centrifuged at 400 g for 180min. Concentrated nanoparticles were then filtered through a 0.22 µm filter and stored at 4 °C.

### LNP characterization

The particle size and polydispersity index of the formulations were obtained using Zetasizer Nano ZS (Malvern Instruments, Malvern, UK) following appropriate dilution in PBS (Supplementary Fig. 1). All measurements were carried out at room temperature.

### Immuno-stimulation assay

THP1-Dual™ cell IRF and NF-κB reporter gene expression were measured as per manufacturer's protocol (InvivoGen, CA). NF-κB and IRF activation pathways were measured by assessing the activity of alkaline phosphatase and luciferase. 2'3'-cGAMP and LPS were obtained from InvivoGen (San Diego, CA).

### In vivo infection and siRNA administration

All animal experiments were performed in compliance with relevant laws and institutional guidelines and in accordance with the ethical standards of the Declaration of Helsinki. For SARS-CoV-2 work, K18-hACE2 mice (3–4 months old) were purchased from the Jackson Laboratory (Bar Harbor, ME) and bred inhouse at the Griffith University Animal Resource Center. Mice were intranasally (IN) infected using the IN instillation technique with  $10^4$ – $10^5$  plaque forming unit (PFU) (20 µL total volume) of live SARS-CoV-2 ancestral strain or delta VOC while under isoflurane anesthesia. Mice were subsequently treated with either naked, sLNP or dmLNP complexed siRNAs retro-orbitally (IV) (100 µL total volume) or IN (20 µL total volume) by IN instillation while

under isoflurane anesthesia. For siRNA dosing on the day of infection (0 days post-infection (dpi)), siRNA was administered 2 h prior to infecting mice with SARS-CoV-2. Mice were monitored daily for weighing and clinical scoring. This work was conducted in a BSL3 approved animal facility at Griffith University (Animal ethics approval: MHIQ/14/21/AEC). For RSV work, BALB/c mice (6–8 weeks old) were purchased from the Animal Resource Center (Perth, Australia). Mice were IN infected with  $10^6$  plaque forming unit (PFU) (20 µL total volume) of live RSV-A2 while under ketamine/xylazine anesthesia. Mice were subsequently treated with either sLNP complexed siRNAs via tail vein injection (IV) (200 µL total volume) or IN (20 µL total volume) while under ketamine/xylazine anesthesia. Cyclophosphamide was administered to mice intraperitoneally (IP) at a single dose of 100 mg/kg five days prior to RSV-A2 infection as previously reported.<sup>13</sup> Mice were monitored daily for weighing and clinical scoring. This work was approved by the Griffith University Animal Ethics Committee (Animal ethics approval: MHIQ/02/14/AEC).

### In vivo biodistribution studies

1,1'-Diocadecyl-3,3,3',3'-tetramethylindotricarbocyanine iodide (DiR) dye was used at a DiR: lipid ratio of 1 in 5400 (w/w) to track the lipid nanoparticles. siGLO Red (Cy3-labelled) transfection indicator (siGLO) was used as an indicator to track the LNP cargo (i.e., siRNA). The biodistribution of DiR-labelled LNP formulations and siGLO encapsulated LNPs were examined in extracted mouse organs on the PhotonIMAGER Optima *in vivo* imager (Biospace Lab, France) at the following wavelengths: excitation 720nm/emission 790 nm for imaging DiR, and excitation 547nm/emission 563 nm for imaging siGLO Red.

### Statistical analysis

All statistical analyses were performed using the statistical software package GraphPad Prism 9 and described in detail in respective figure legends.

## Results and discussion

We have previously demonstrated highly potent *in vitro* and *in vivo* targeting of SARS-CoV-2 Wuhan (ancestral) strain with siRNAs targeting the ultra-conserved regions in the helicase (siHel2), and untranslated region (siUTR3).<sup>7</sup> Here, we tested these siRNAs against all SARS-CoV-2 variants of concern (VOC) and find that they are equipotent *in vitro* (Fig. 1A). Next, we wanted to determine whether the potent antiviral effect observed previously with these siRNAs *in vivo* can be recapitulated in mice infected with another SARS-CoV-2 VOC. In contrast to the B.1.1.529 (omicron) SARS-CoV-2 infection model (Supplementary Fig. 2), we were able to detect lung viral loads at 3 days post infection (dpi) in the B.1.617.2 (delta) SARS-CoV-2 infection model (Supplementary Fig. 3). Though the lack of clinical disease (i.e., weight change) in our omicron SARS-CoV-2 infection model is consistent with what was observed by others,<sup>14</sup> we were unable to detect measurable lung infection at 3dpi. We speculate that omicron SARS-CoV-2 infection in younger mice (3–4 months old),

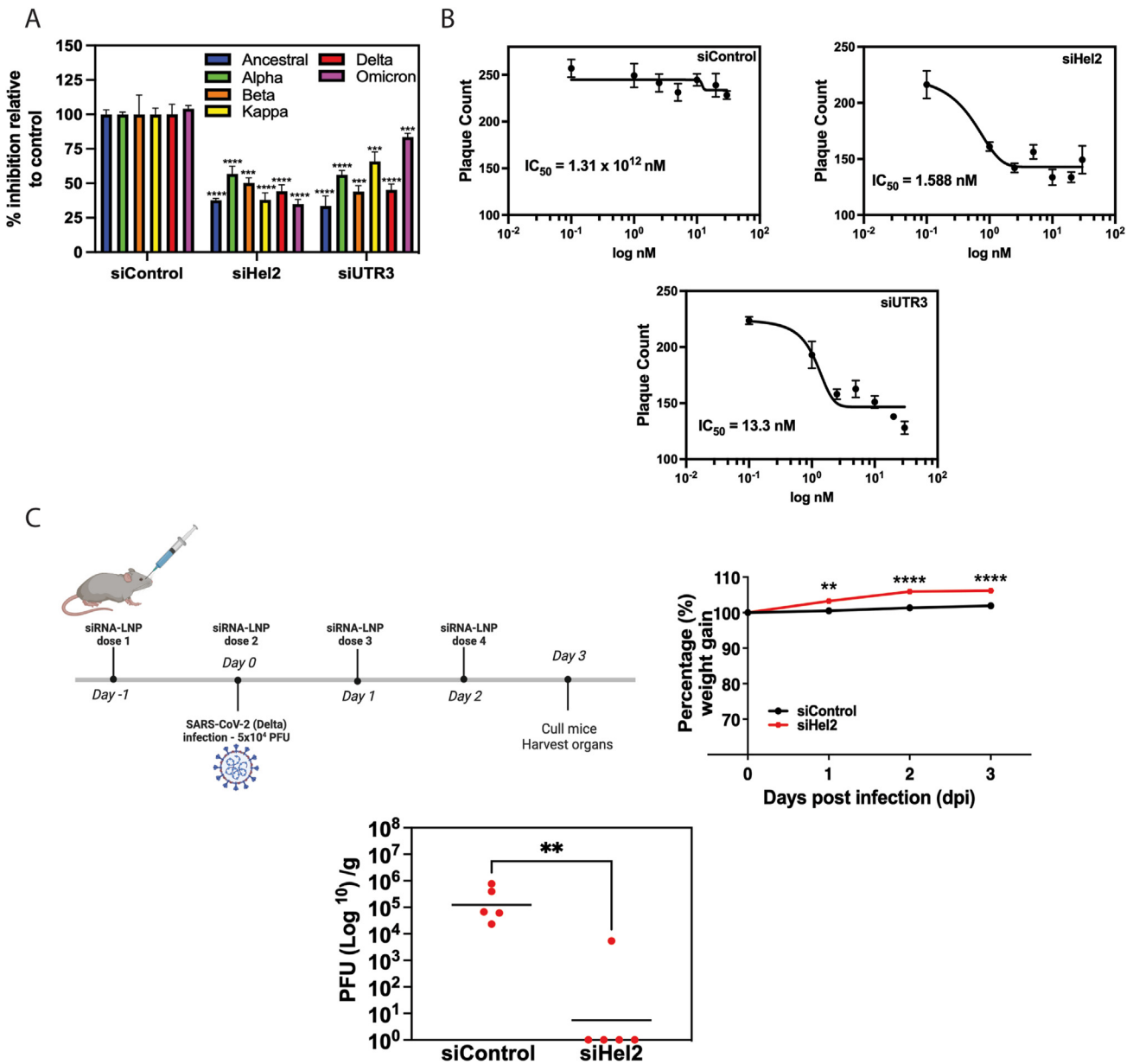


**Figure 1.** SARS-CoV-2 targeting siRNAs are effective at reducing lung viral infection *in vivo*. A) Vero E6 cells were transfected with control and targeting siRNAs (30 nM) complexed to Lipofectamine 2000 for 24 h before infecting with indicated SARS-CoV-2 VOC at 250 plaque forming unit (PFU). Infectious viral plaques were counted 4 days post infection (dpi). Data is expressed as mean percentage plaque inhibition relative to virus alone (control) and is representative of the standard error of the mean (SEM) of triplicate treatments. \*\*\* $p < 0.001$  and \*\*\*\* $p < 0.0001$ , one-way ANOVA (Dunnett’s post-test) when compared against siControl. The control siRNA used here is siN367 (siControl). Data is representative of one out of three independent experiments. B) Vero E6 cells were transfected with increasing concentrations (0.1–30 nM) of control and targeting siRNAs complexed to Lipofectamine 2000 for 24 h before infecting with delta SARS-CoV-2 VOC at 250 PFU. Infectious viral plaques were counted 4dpi. Data is expressed mean plaque counts and standard error of the mean (SEM) of triplicate treatments and IC<sub>50</sub> determined using the statistical software package GraphPad Prism 9. C) K18h-ACE2 mice infected with  $5 \times 10^4$  live delta SARS-CoV-2 VOC received daily intravenous (IV) (retro-orbital) treatment of siRNA-sLNP (1 mg/kg) daily (–1 to 2 dpi). The control siRNA used here is siN367 (siControl). Lung viral tissue counts/g at 3dpi are shown. Each dot represents data from one mouse and bars represent the mean. \*\* $p < 0.005$  one-way ANOVA (Dunnett’s post-test). Mice were weighted daily, and data points denote mean percentage weight gain and error bars represent SEM. \*\* $P < 0.01$ , \*\*\*\* $P < 0.0001$ , Two-way ANOVA.

as opposed to older mice (5–6 months old),<sup>14</sup> would result in detectable lung infection. Hence, we decided to test our siRNAs in a delta SARS-CoV-2 infection model in all our *in vivo* experiments. Given that siHel2 exhibited a lower IC<sub>50</sub> than

siUTR3 against the delta variant (Fig. 1B), we complexed siHel2 with stealth LNPs (sLNPs) for IV administration, parallel to what we did previously for targeting SARS-CoV-2 ancestral strain *in vivo*.<sup>7</sup> LNP systems are typically

composed of a zwitterionic lipid, an ionizable cationic lipid, poly(ethylene glycol)-lipid (PEG-lipid), cholesterol, and the nucleic acid cargo. Unlike standard liposomes, we have developed sLNPs that are specifically formulated to be stable in serum, circulate for long periods, and protect siRNA payloads from nucleases.<sup>12,15</sup> Consistent with our previous observations,<sup>7</sup> prophylactic administration of siHel2-sLNP via IV administration results in almost complete amelioration of viral infection in mice lungs (Fig. 1C).

Meyers et al.,<sup>16</sup> previously screened a range of siRNAs targeting the phosphoprotein (P), N and large (L) protein genes and showed varying silencing potency against the RSV-A2 strain. Notably, the siRNA targeting the P gene (siP) exhibited over 95% inhibition at a concentration of 5 nM. As was done previously with SARS-CoV-2 targeting siRNAs, siHel2 and siUTR3,<sup>7</sup> we converted RSV-targeting siRNA, siP, into dicer substrate-siRNA (D-siRNA) for more potent target mRNA silencing (Table 1) and verified the ability for siP to reduce RSV infection and RSV P gene expression *in vitro* (Supplementary Fig. 4). LNPs have been shown to functionally deliver nucleic acid payloads to the lung following IN administration.<sup>17</sup> We postulate that IN administration of RSV-targeting siRNAs complexed in sLNPs would functionally repress RSV infection in mouse lungs. Here, siP is complexed into sLNP (siP-sLNP), as we have done previously for *in vivo* siRNA-specific SARS-CoV-2 lung targeting via the IV route.<sup>7</sup> Indeed, prophylactic IV and IN administration of siP-sLNP resulted in significant reduction of lung viral load in RSV-A2 infected BALB/c mice at 3 days post-infection (dpi) (Fig. 2A). Remarkably, we observed a similar effect with a therapeutic intervention regimen at 7dpi in mice pre-treated with cyclophosphamide (Fig. 2B). Pre-treatment of BALB/c mice with cyclophosphamide, rendering the mice in an immunocompromised state, results in a more severe and sustained RSV *in vivo* infection model.<sup>13</sup> Overall, both therapeutic and prophylactic IN and IV administration of RSV-targeting siRNA packaged into sLNPs results in the reduction of RSV lung infection *in vivo*. IN delivery of unmodified anti-RSV siRNA targeting the P gene have been attempted previously *in vivo* and resulted in effective reduction of RSV lung infection.<sup>18</sup> Unmodified siRNAs are siRNAs that have not undergone necessary chemical modifications to protect it from nuclease degradation. It is important to note that the study administered almost double the amount of siRNA (70 µg siRNA) we used here (40 µg siRNA) and without the aid of a carrier system (e.g., LNPs). We speculate that this was to compensate for any loss of siRNA bioactivity due to their unmodified siRNAs becoming prone to nuclease degradation over time. Nonetheless, we show that targeting the RSV P gene prophylactically and therapeutically using targeting siRNAs encapsulated in sLNP can reduce RSV lung infection.

We have previously used LNP formulations composed of DOTAP with the ionizable lipid DLin-MC3-DMA (dmLNP)<sup>19</sup> and observed that both sLNPs and dmLNPs efficiently deliver siRNAs to the lungs of CoV-2-infected mice via IV administration.<sup>7</sup> Interestingly, we observed that dmLNPs had better lung biodistribution than sLNPs when delivered via the IN route (Fig. 3A) and that the majority of siRNA payload end up in the lungs compared to the nasal cavity when formulated with dmLNP (Fig. 3B). Hence, we wanted to test this LNP formulation in an *in vivo* SARS-CoV-2 infection model by

packaging siHel2 and siUTR3 in dmLNPs for IN delivery. We confirmed that dmLNPs alone or formulated with target siRNAs were not immunostimulatory (Supplementary Fig. 5). Prophylactic IN administration of both SARS-CoV-2 targeting siRNA-dmLNPs reduced delta SARS-CoV-2 lung load but the effect was most significant with siUTR3 48 h after the last siRNA dose (Fig. 3C). We attribute this moderate effectiveness to the lack of siRNA biodistribution in mice the lungs at 48 h post-IN delivery of siRNA-dmLNPs (Fig. 3B). Despite this, the observations suggest that strong anti-SARS-CoV-2 siRNA potency can be maintained *in vivo*, underscoring the effectiveness of siRNA-dmLNPs delivered via the IN route. Next, we then wanted to determine whether the observed anti-SARS-CoV-2 effect can be maintained when delivered without siRNA-dmLNP encapsulation. Notably, the previously observed antiviral effect was lost when siUTR3 was delivered unencapsulated (naked) by the IN route (Fig. 3D). Though not significant, chemically modifying siUTR3 with 2'O-methyl and phosphorothioate modifications (siMod-UTR3), which have previously been shown to enhance siUTR3 stability and protection from nuclease degradation,<sup>7</sup> maintained anti-SARS-CoV-2 effectiveness *in vivo* (Fig. 3D). This data suggests that LNPs are important in protecting siRNAs and anti-SARS-CoV-2 activity *in vivo*. Indeed, Chang et al.,<sup>9</sup> demonstrated lung anti-SARS-CoV-2 effect of IN-delivered chemically modified naked siRNAs *in vivo*, emphasizing the need to chemically modify siRNAs when delivering without a carrier vessel. Collectively, we find here that prophylactic IN administration of siRNA-dmLNPs can effectively reduce SARS-CoV-2 lung infection *in vivo*. It is important to note that better lung antiviral activity is observed when siRNA-LNPs were delivered by IV (Fig. 1C), consistent with what was previously observed.<sup>7</sup> Indeed, IV delivered sLNP<sup>15</sup> and dmLNP<sup>7</sup> have been shown to efficiently target the lungs *in vivo*. The observation with IN delivered siRNA-LNPs (Fig. 3C) is unsurprising as IN delivery of LNPs is challenging as LNPs must travel and penetrate respiratory mucosal barriers to reach the lungs, rather than via the bloodstream (i.e., via IV). Future work will endeavour to address this challenge by changing the method of IN delivery (i.e., IN instillation) by aerosolizing siRNA-LNP complexes, a method previously used for delivering naked siRNAs,<sup>9</sup> for better respiratory delivery.

The impact of emerging respiratory virus infections in humans is not trivial. Indeed, there is currently a need for the development of antiviral RNA therapeutics to control virus infections especially those with pandemic capacity. A modular therapeutic platform that can treat respiratory RNA viruses, as well as their emerging variants could not only be paradigm shifting in the management of pandemics, but also in the preparedness for future pandemics. Additionally, there is an urgent need for new platforms that enhance RNA therapeutic efficacy, bioavailability and biodistribution. Importantly, siRNA delivery into the lower respiratory tract via the IN route poses several challenges (e.g., nasal mucosal barriers). While IV works to deliver siRNA to the lungs,<sup>7</sup> it is not a practical approach nor amendable in a clinical outpatient setting. A more practical approach to deliver siRNA is by direct inhalation and/or nebulization. Here, we utilize LNPs as effective carrier vessels for siRNAs delivered via the IN route and showed that SARS-CoV-2 and RSV-targeting siRNAs were efficacious

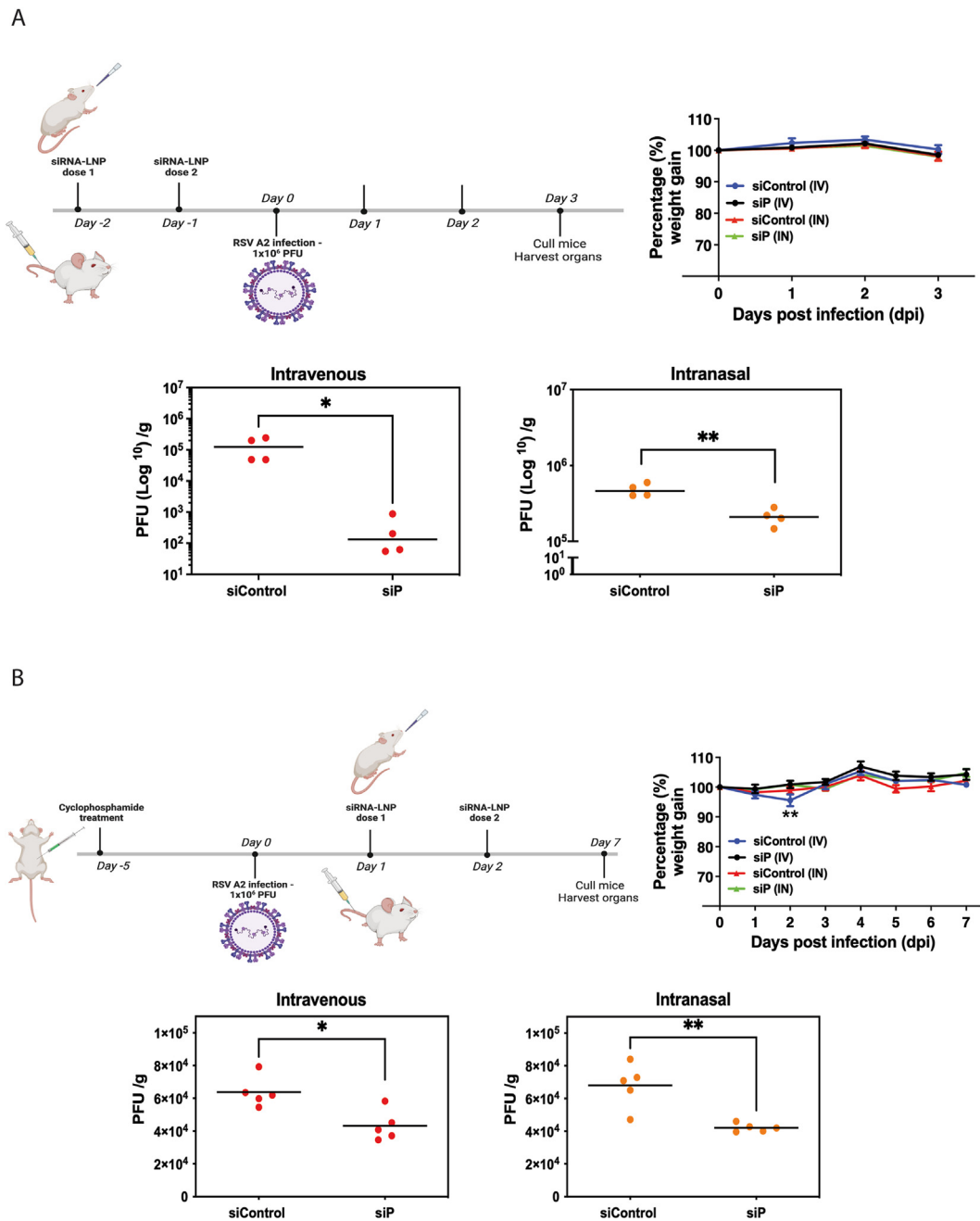


**Figure 2. RSV targeting siRNAs are effective at reducing lung viral infection *in vivo*.** A) BALB/c mice infected with  $1 \times 10^6$  live RSV-A2 received either IV (tail vein) or intranasal (IN) treatment of siRNA-sLNP ( $40 \mu\text{g}$  siRNA) every 24 h ( $-2$  to  $-1$ dpi). The control siRNA used here is siScrM7 (siControl). Lung viral tissue counts/g at 3dpi are shown. Each dot represents data from one mouse and bars represent the mean.  $*p < 0.05$ ,  $**p < 0.005$  one-way ANOVA (Dunnnett's post-test). Mice were weighted daily, and data points denote mean percentage weight gain and error bars represent SEM.  $**P < 0.01$ , Two-way ANOVA only revealed a significant difference between siControl and siP in the IV administered group at 2dpi. B) BALB/c mice infected with  $1 \times 10^6$  live RSV-A2 received either IV (tail vein) or intranasal (IN) treatment of siRNA-sLNP ( $40 \mu\text{g}$  siRNA) every 24 h (1 to 2dpi). The control siRNA used here is siGFP (siControl). Cyclophosphamide was administered to mice intraperitoneally (IP) ( $100 \text{ mg/kg}$ ) at  $-5$ dpi. Lung viral tissue counts/g at 7dpi are shown. Each dot represents data from one mouse and bars represent the mean.  $*p < 0.05$ ,  $**p < 0.005$  one-way ANOVA (Dunnnett's post-test). Mice were weighted daily, and data points denote mean percentage weight gain and error bars represent SEM.

in infected mouse lungs. It is important to note that we observed this antiviral effect to a lesser degree in RSV infected mice than in SARS-CoV-2 infected mice. Unlike anti-SARS-CoV-2 siRNAs (Fig. 3), anti-RSV siRNAs were

formulated in sLNPs (Fig. 2). Given that IN administered dmLNPs resulted in better siRNA lung biodistribution than sLNP (Fig. 3A), we speculate that an improved anti-RSV effect would be observed if dmLNPs were used. Future

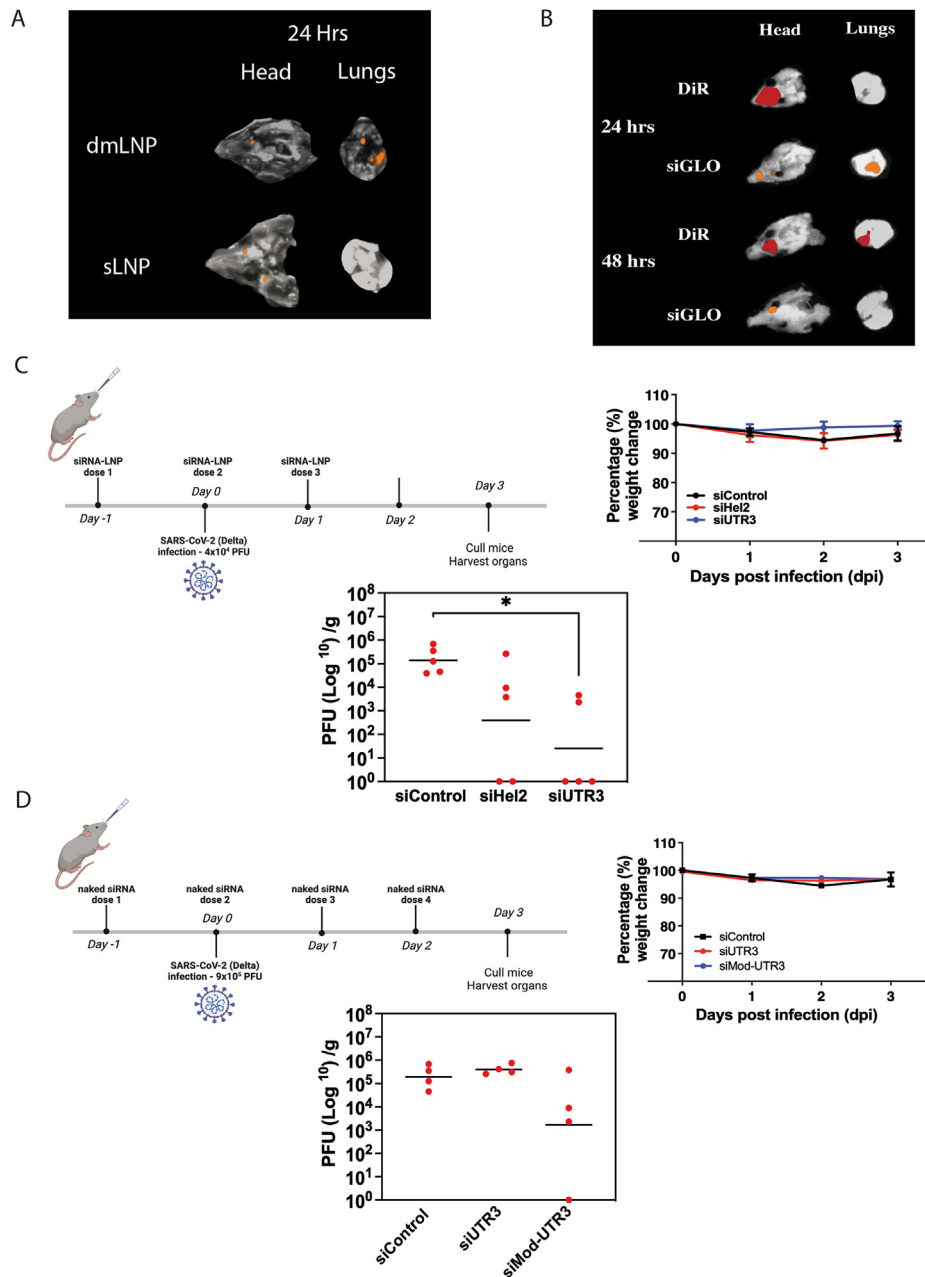


**Figure 3.** Intranasal delivery of SARS-CoV-2 targeting siRNAs reduces viral lung loads *in vivo*. A) K18hACE2 mice received either siGLO-dmLNP (1 mg/kg) or siGLO-sLNP (1 mg/kg) via IN treatment and organs harvested at various time points before measuring fluorescence on the PhotonIMAGER Optima *in vivo* imager. B) K18hACE2 mice received siGLO-dmLNP (1 mg/kg) or dmLNP-loaded with fluorescent DiR via IN treatment and organs harvested at various time points before measuring fluorescence on the PhotonIMAGER Optima *in vivo* imager. C) K18h-ACE2 mice infected with  $4 \times 10^4$  live delta SARS-CoV-2 VOC received daily IN treatment of siRNA-dmLNP (1 mg/kg) daily (–1 to 1dpi). The control siRNA used here is siN367 (siControl). Lung viral tissue counts/g at 3dpi are shown. Each dot represents data from one mouse and bars represent the mean. \* $p < 0.05$  one-way ANOVA (Dunnett’s post-test). Mice were weighted daily, and data points denote mean percentage weight gain and error bars represent SEM. D) K18h-ACE2 mice infected with  $9 \times 10^5$  live delta SARS-CoV-2 VOC received daily IN treatment of unencapsulated (naked) siUTR3, siMod-UTR3 (1 mg/kg) or siControl-dmLNP (1 mg/kg) daily (–1 to 2dpi). The control siRNA used here is siN367 (siControl). Lung viral tissue counts/g at 3dpi are shown. Each dot represents data from one mouse and bars represent the mean. Mice were weighted daily, and data points denote mean percentage weight gain and error bars represent SEM.

work will focus on testing dmLNP-siP formulations for RSV *in vivo* work. It is also interesting that sustained dmLNP-siRNA biodistribution was observed in the nasal cavity (Fig. 3B). Despite this, we fail to see any anti-SARS-CoV-2

effect in the nasal cavity (Supplementary Fig. 6). We suspect that poor penetration through the nasal mucosal barrier may be hindering siRNA payload from reaching target nasal epithelial cells. Future work will focus on



improving this by designing LNPs and IN delivery methods that can penetrate the nasal mucosal barrier for both RSV and SARS-CoV-2 infection models. Another limitation in this work is the inability to conduct *in vivo* testing in an omicron SARS-CoV-2 infection model. We plan to continue this work in future studies using an improved omicron *in vivo* model by recapitulating the same conditions (i.e., 5–6 month old mice) Halfmann et al.,<sup>14</sup> used in their study. However, the omicron *in vivo* mouse model remains a poor model to study any impact our siRNA treatment may have at reducing clinical disease as these omicron VOC infected mice do not present clinical disease (i.e., no weight loss)<sup>14</sup> (Supplementary Fig. 2). Our current work also only tested the effect of prophylactically treating mice with siRNAs and measuring antiviral effect after 3 days post-infection. Hence, we were unable to report late-stage clinical survival with our siRNA treatments as clinical symptoms (i.e., weight loss) only appear after 3dpi in the delta *in vivo* infection model (Supplementary data 3). Despite this, we did observe significant weight gain in the siHel2 treatment group relative to siControl group when delivered by IV (Fig. 1C). We have only tested a post-exposure therapeutic intervention in a cyclophosphamide-treated RSV infection model to assess the long-term impact of siRNA therapy in an immunocompromised animal model (Fig. 2B). We only observed significant clinical improvement at 2dpi with an IV intervention but marginal though significant decrease in lung infection with both IV and IN interventions at 7dpi. We speculate that more repeated siRNA-LNP doses could improve both lung antiviral effects and clinical disease. Our future work plans to extend this study to test both prophylactic and therapeutic IN siRNA treatment regimens and assessing clinical disease improvement over a period of 7 days or longer.

siRNAs are highly specific to their targets and are now in the clinic for several human disorders.<sup>20</sup> For example, siRNA therapeutics developed by Alnylam Pharmaceuticals, patisiran (IV administered) and givosiran (subcutaneously administered), were both approved by the FDA in recent years to treat polyneuropathy. However, we are yet to see an approved inhalable siRNA therapeutic product, possibly due to the inherent challenges associated with this mode of delivery (i.e., effective biodistribution and mechanical method for administering an inhaled drug).<sup>21</sup> Though we show that prophylactic IN delivered LNP encapsulated siRNAs is effective in respiratory virus infection models, whether these siRNA-LNPs can be aerosolized and maintain bioactivity in lungs thereafter has yet to be determined. Nonetheless, the data presented here sets precedence for delivering siRNA molecules using the LNP platform via the IN route for effective targeting of emerging respiratory viral infections in the lower respiratory tract.

## Ethics approval statement

All animal experiments were performed in compliance with relevant laws and institutional guidelines and in accordance with the ethical standards of the Declaration of Helsinki. All work was approved by the Griffith University Animal Ethics Committee (Animal ethics approval: MHIQ/02/14/AEC and MHIQ/14/21/AEC).

## Funding statement

This work was supported by the NHMRC Project Grant (APP1047635) to N.A.J.M.

## Disclosure of conflicts of interest

Y.T is the founding director for Prorenata Biotech. N.A.J.M and K.V.M are both consultants for Prorenata Biotech.

## Declarations of interest

K.V.M. has submitted provisional patent 048440-762P02US on the technologies reported here.

## Acknowledgements

We would like to thank Dr Naphak Modhiran and Associate Professor Dan Watterson (School of Chemistry and Molecular Biosciences, The University of Queensland, QLD, Australia) for providing us with SARS-CoV-2 (CR3022) recombinant monoclonal antibodies. We would also like to thank Professor Paul Young (School of Chemistry and Molecular Biosciences, The University of Queensland, QLD, Australia) for providing us with RSV-A2 and anti-RSV sera and the Peter Doherty Institute for Infection and Immunity and Melbourne Health, Victoria, Australia for providing us with SARS-CoV-2 VOCs.

## References

1. Organization GWH. *WHO COVID-19 dashboard*. 2020 (last cited: 20/07/2022).
2. Behzadi MA, Leyva-Grado VH. Overview of current therapeutics and novel candidates against influenza, respiratory syncytial virus, and Middle East respiratory syndrome coronavirus infections. *Front Microbiol* 2019;10.
3. Jayk Bernal A, Gomes da Silva MM, Musungaie DB, Kovalchuk E, Gonzalez A, Delos Reyes V, et al. Molnupiravir for oral treatment of covid-19 in nonhospitalized patients. *N Engl J Med* 2022;386:509–20.
4. Corbett KS, Edwards DK, Leist SR, Abiona OM, Boyoglu-Barnum S, Gillespie RA, et al. SARS-CoV-2 mRNA vaccine design enabled by prototype pathogen preparedness. *Nature* 2020; 586:567–71.
5. Sasso JM, Ambrose BJB, Tenchov R, Datta RS, Basel MT, DeLong RK, et al. The progress and promise of RNA medicine horizontal line an arsenal of targeted treatments. *J Med Chem* 2022;65:6975–7015.
6. Chi X, Gatti P, Papoian T. Safety of antisense oligonucleotide and siRNA-based therapeutics. *Drug Discov Today* 2017;22: 823–33.
7. Idris A, Davis A, Supramaniam A, Acharya D, Kelly G, Tayyar Y, et al. A SARS-CoV-2 targeted siRNA-nanoparticle therapy for COVID-19. *Mol Ther* 2021;29:2219–26.
8. DeVincenzo J, Cehelsky JE, Alvarez R, Elbashir S, Harborth J, Toudjarska I, et al. Evaluation of the safety, tolerability and pharmacokinetics of ALN-RSV01, a novel RNAi antiviral therapeutic directed against respiratory syncytial virus (RSV). *Antivir Res* 2008;77:225–31.
9. Chang, Y.-C., Yang, C.-F., Chen, Y.-F., Yang, C.-C., Chou, Y.-L., Chou, H.-W. *et al.* A siRNA targets and inhibits a broad range of

- SARS-CoV-2 infections including Delta variant. *EMBO Molecular Medicine* n/a, e15298.
10. Khaitov M, Nikonova A, Shilovskiy I, Kozhikhova K, Kofiadi I, Vishnyakova L, et al. Silencing of SARS-CoV-2 with modified siRNA-peptide dendrimer formulation. *Allergy* 2021;76:2840–54.
  11. Amarilla AA, Modhiran N, Setoh YX, Peng NYG, Sng JDJ, Liang B, et al. An optimized high-throughput immuno-plaque assay for SARS-CoV-2. *Front Microbiol* 2021;12:625136.
  12. Wu SY, Putral LN, Liang M, Chang H-I, Davies NM, McMillan NAJ. Development of a novel method for formulating stable siRNA-loaded lipid particles for in vivo use. *Pharmaceut Res* 2008;26:512.
  13. Kong X, Hellermann GR, Patton G, Kumar M, Behera A, Randall TS, et al. An immunocompromised BALB/c mouse model for respiratory syncytial virus infection. *Virology* 2005;2:3.
  14. Halfmann PJ, Iida S, Iwatsuki-Horimoto K, Maemura T, Kiso M, Scheaffer SM, et al. SARS-CoV-2 Omicron virus causes attenuated disease in mice and hamsters. *Nature* 2022;603:687–92.
  15. McCaskill JL, Marsh GA, Monaghan P, Wang LF, Doran T, McMillan NA. Potent inhibition of Hendra virus infection via RNA interference and poly I:C immune activation. *PLoS One* 2013;8:e64360.
  16. Meyers R, Alvarez R, Tripp R, Hadwiger P, Constein R, Elbashir S, et al. ALN-RSV01, an RNAi therapeutic for the treatment of respiratory syncytial virus (RSV) infection. *E-Pediatr Acad Soc* 2007;616295.
  17. Liang W, Pan HW, Vllasaliu D, Lam JKW. Pulmonary delivery of biological drugs. *Pharmaceutics* 2020;12.
  18. Bitko V, Musiyenko A, Shulyayeva O, Barik S. Inhibition of respiratory viruses by nasally administered siRNA. *Nat Med* 2005;11:50–5.
  19. Cheng Q, Wei T, Farbiak L, Johnson LT, Dilliard SA, Siegwart DJ. Selective organ targeting (SORT) nanoparticles for tissue-specific mRNA delivery and CRISPR-Cas gene editing. *Nat Nanotechnol* 2020;15:313–20.
  20. Hu B, Zhong L, Weng Y, Peng L, Huang Y, Zhao Y, et al. Therapeutic siRNA: state of the art. *Signal Transduct Targeted Ther* 2020;5:101.
  21. Shaffer C. Mist begins to clear for lung delivery of RNA. *Nat Biotechnol* 2020;38:1110–2.

## Appendix A. Supplementary data

Supplementary data to this article can be found online at <https://doi.org/10.1016/j.jmii.2023.02.010>.